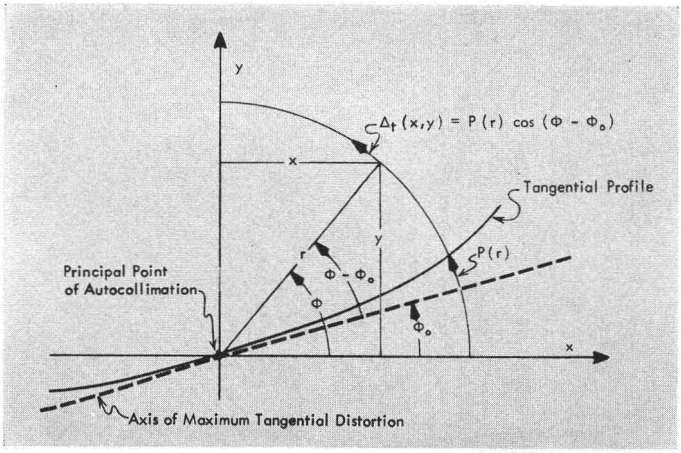

FIG. 1. Illustrating geometrical significance of parameters defining tangential distortion according to thin prism model.

DUANE C. BROWN*
D. Brown Associates, Inc.
Eau Gallie, Florida

Decentering Distortion of Lenses

The prism effect encountered in metric cameras can be overcome through analytic calibration.

INTRODUCTION

THE DISTORTION of a perfectly centered lens composed of individually flawless elements is strictly symmetric about the optical axis. A significant degree of decentering will introduce both tangential distortion and asymmetric radial distortion. The physical suppression of such distortion to a value not exceeding five microns over the plate format of the typical mapping camera requires appreciable skill and patience on the part of the optical technician in aligning the lens; its suppression to less than two microns calls for luck in addition to skill and patience. In view of the increasingly stringent requirements for calibration resulting from recent advances in analytical photogrammetric triangulation, it is no longer tenable to ignore or dismiss the metric consequences of decentering distortion of even exceptionally well centered lenses.

In this paper we shall review the general problem of decentering distortion, consider its analytical representation, establish its projective properties, and demonstrate the practicality of its precise calibration. In doing so, we shall review and partially reconcile two apparently conflicting theories of decentering distortion: the thin prism model and Conrady's model. We shall also provide experimental verification of our major findings. The present paper is in large measure a revision and extension of a section of an earlier paper (Brown, 1964; Section 10: Calibration of Distortion Caused by Lens Decentration).

THE THIN PRISM MODEL

According to the thin prism model, the distortion introduced by a slightly decentered

* Presented at the Annual Convention of the American Society of Photogrammetry, Washington, D. C., March 1965, under the title "Decentering Distortion and the Definitive Calibration of Metric Cameras."

lens can very nearly be duplicated by placing an appropriately oriented thin prism of appropriate deviation in front of a perfectly centered lens. In general, a single such prism is adequate to account for the composite effect of any number of decentered elements, for a group of individual prisms in object space (one associated with each decentered element) can be replaced by a single, equivalent prism. In reviewing both the photogrammetric and the optical literature, we have found that with but one notable exception ment with what was to be expected from the thin prism model. The thin prism model was adopted by Sharp (1949) in his consideration of the consequences of tangential distortion occuring in multiplex projectors and by Sewell (1952) in his treatment of camera calibration in the ASP Manual of Photogrammetry. Washer (1941) adopted the thin prism model in considering the effects of decentering (or of a bent optical axis) on the physical determination of the principal point. Later, in a comprehensive experimental investigation of

ABSTRACT: *The thin prism model has been widely adopted in the photogrammetric literature to describe the effects of a sensibly decentered lens. Exact expressions are derived for the radial and tangential components of the distortion introduced by a thin prism placed in front of a perfectly centered lens. This model is compared with an alternative model (Conrady, 1919) based on rigorous analytical ray tracing through a decentered lens. When the principal point of autocollimation is adopted as the plate origin, the two models are found to be in precise agreement regarding the tangential component of decentering distortion, but are found to be at variance by a factor of three regarding the radial component. However, when compensatory translation of the plate and tipping of the camera are permitted to operate, the two models are found to be projectively equivalent to terms of leading order. Because this projective equivalence does not extend to higher order effects (which may assume prominence with wide angle cameras), Conrady's model is clearly to be preferred for general application. An extended form of Conrady's model has been put to practical application in the stellar calibration of ballistic cameras. Results of actual calibrations are presented and discussed, and the implications of the present development to analytical photogrammetry are examined.*

(Conrady, 1919) the thin prism model appears to have been almost universally adopted to account for decentering distortion.

The few textbooks on optics according any consideration at all to decentered lenses invoke the thin prism model with little or no special justification (Hardy and Perrin, 1932; Strong, 1958; Martin, 1948). The same is true throughout the photogrammetric literature. Bennett (1927) was one of the earliest to resort to the thin prism model to explain the tangential distortion observed in a number of lenses. Pennington (1947) noted the systematic effects of tangential distortion on photogrammetric extension of control and discussed the practical determination of tangential distortion, pointing out that its observed characteristics are in general agree-

thin prism distortion Washer (1957 a, b) photographed target arrays both with and without a thin prism of known deviation placed in front of a well centered lens. He was thereby able to demonstrate explicitly that significant asymmetric radial effects are to be expected from thin prism distortion in addition to the tangential effects considered by other investigators.

It should be noted, however, that the radial effects of decentering distortion had been implicitly taken into consideration, in an investigation performed by Carman (1948). In this investigation sets of rays from points on a uniform grid in object space were numerically traced through a thin prism placed in front of a hypothetical mapping camera. Carman was thereby able to demonstrate

that a suitable choice of principal point can significantly reduce, though not eliminate, the effects of thin prism distortion.

It is well to consider at this point the precise behavior of tangential distortion according to the thin prism model. As described by Pennington (1947) there exists in the image plane an axis passing through the principal point along which the tangential distortion is maximum (the term principal point is used here in a loose sense). There also exists in the image plane an axis through the principal point along which the tangential distortion is zero. The axis of zero tangential distortion is orthogonal to the axis of maximum tangential distortion. The tangential distortion along any other axis passing through the principal point and lying in the image plane is proportional to that along the axis of maximum tangential distortion, the constant of proportionality being the cosine of the angle between the two axes. In analytical terms, the thin prism model for tangential distortion may be expressed as

$$\Delta_t(x, y) = P(r) \cos(\phi - \phi_0)$$
$$= \left(\frac{x}{r} \cos\phi_0 + \frac{y}{r} \sin\phi_0\right) P(r) \quad (1)$$

in which

$\Delta_t(x,y)$ = tangential distortion at x, y in image plane (origin taken at principal point of autocollimation),
$r = (x^2+y^2)^{1/2}$ = radial distance,
$P(r)$ = tangential profile (tangential distortion at radial distance r along axis of maximum tangential distortion),
ϕ_0 = angle between positive x-axis and axis of maximum tangential distortion (see Figure 1),
ϕ = angle between positive x-axis and radius vector from origin to x, y.

At the principal point the tangential profile $P(r)$ is zero and is tangent to the axis of maximum tangential distortion.

Using the method suggested by Pennington, Livingston (1951) measured tangential distortion across both diagonals of the photographic format of a total of 33 Metrogon lenses and one Topogon. As we shall presently see, Livingston's results are not generally in strict accord with the thin prism model for angles in excess of about 25° from the axis of the camera. However, they do substantiate the "cosine variation" of tangential distortion in accordance with Equation 1.

Exact Analytical Expressions for Thin Prism Distortion

Despite the widespread adoption of the thin prism model, we have been unable to find in the literature exact analytical expressions defining the precise relationship between the radial and tangential distortion induced by a thin prism at any specified azimuth. Washer's (1957 a, b) explicit results, for instance, are restricted to the plane through the principal section of the prism and to the plane normal to the principal section (both planes contain the optical axis); his discussion of azimuthal variation is brief and is strictly qualitative, apparently being based on limited experimental findings rather than on detailed analytical results. In order to shed light on this matter, we have performed exact analytical, three-dimensional ray tracing through a thin prism. The key results of this investigation as reported in our earlier paper (Brown, 1964) are as follows. The radial and tangential components of thin prism distortion of an image of plate coordinates x, y are given by

$$\Delta_r(x, y) = P \cos(\phi - \phi_0),$$
$$\Delta_t(x, y) = P \sin(\phi - \phi_0), \quad (2)$$

in which

$$P = c[\,(\cos\theta_1 \cos\mu\epsilon - \cos\theta_3) \sin\mu\epsilon$$
$$+ (1 - \cos\epsilon \cos\mu\epsilon) \sin\theta_0 \sin(\phi - \phi_0)\,] \quad (3)$$

where

c = principal distance (same units as x, y),
ϵ = angle of prism (radians),
μ = index of refraction of prism,
ϕ = angle between radius vector to x, y and positive x-axis,
ϕ_0 = angle between positive x-axis and image of edge of prism (if $\phi = 0°$, a line that is normal to the image of the apex of the prism and is directed through the principal point coincides with the positive y-axis; if $\phi_0 = 180°$, such a line coincides with the negative y-axis),
θ_0 = angle between undeviated principal axis and ray to image point (undeviated principal axis is arbitrarily taken to be normal to front surface of prism),
θ_1 = angle between principal ray and image ray after refraction by first surface of prism,
θ_2 = angle between normal to second surface of prism and refracted ray within prism,
θ_3 = angle between emergent ray and normal to rear surface of prism.

For specified c, μ, ϵ and ϕ_0 the various quantities appearing in Equation 2 can be computed from the plate coordinates x, y by means of the following sequence of equations:

$$\begin{aligned} r &= (x^2 + y^2)^{1/2} \\ \sin\theta_0 &= r/(r^2 + c^2)^{1/2} \\ \sin\phi &= x/r \\ \cos\phi &= y/r \\ \sin\theta_1 &= (\sin\theta_0)/\mu \\ \cos\theta_2 &= \sin(\phi - \phi_0)\sin\theta_1 \sin\epsilon + \cos\theta_1\cos\epsilon \\ \sin\theta_3 &= \mu\sin\theta_2. \end{aligned}$$

It is to be emphasized that the above expressions for P and for $\Delta_r(x, y)$, $\Delta_t(x, y)$ are exact; no approximations were resorted to in their derivation.

Properties of Thin Prism Distortion

If ϵ is regarded as a small angle and only first order terms are retained, P can be reduced to the form

$$P = (c\mu\epsilon)(\cos\theta_1 - \cos\theta_3). \tag{4}$$

This in turn can be expanded to either of the following:

$$\begin{aligned} P &= \frac{c\mu\epsilon}{2}\left(1 - \frac{1}{\mu^2}\right)\sin^2\theta_0 \\ &\quad + \text{higher order terms in } \phi \text{ and powers of } \sin^2\theta_0 \\ P &= \frac{\mu\epsilon}{2c}\left(1 - \frac{1}{\mu^2}\right)r^2 \\ &\quad + \text{higher order terms in } \phi \text{ and powers of } r^2. \end{aligned} \tag{5}$$

These equations demonstrate that to terms of leading order neither μ nor ϵ is individually of consequence, but rather that both combine to form the essential parameter of the prism which is expressed by the common factor in the cofficients of $\sin^2\theta_0$ and r^2. Accordingly, insofar as the tangential profile is concerned, there exist families of projectively equivalent thin prisms and one is at liberty to assign any value such that $\mu > 1$ and $\epsilon > 0$ for either μ or ϵ, but not for both simultaneously. In practice, it is convenient to specify a fixed value for μ that is typical for glass and to let ϵ assume the role of the free parameter. The value $\mu = \sqrt{2}$, though slightly low for normal glasses, has been used in our studies because it lends some simplification to the ray tracing equations. Washer (1957 a, b) adopts the value $\mu = 1.5$.

The explicit formulation provided by Equations 2 shows clearly that the radial and tangential components of thin prism distortion are of essentially equal magnitude at equal radial distances along orthogonal radii. From the ray tracing equations it is clear that θ_2 and hence θ_3 are weakly dependent on the azimuth ϕ. This means that even in the simplified Expression 4, the profile function P is not strictly a function of radial distance (or of θ_0) but varies weakly with ϕ as well. However, for small ϵ this dependence of P on ϕ is negligible for all practical purposes.

The general relationships between the x, y components (Δ_x, Δ_y) of distortion and the radial and tangential components (here denoted more compactly by Δ_r, Δ_t) are given by

$$\begin{aligned} \Delta_x &= \Delta_r\cos\phi - \Delta_t\sin\phi, \\ \Delta_y &= \Delta_r\sin\phi + \Delta_t\cos\phi. \end{aligned}$$

From these and Equation 2 it follows that the x, y components of thin prism distortion are

$$\begin{aligned} \Delta_x &= -P\sin\phi_0, \\ \Delta_y &= P\cos\phi_0. \end{aligned} \tag{6}$$

It follows that

$$P = (\Delta_x^2 + \Delta_y^2)^{1/2} = (\Delta_r^2 + \Delta_t^2)^{1/2} \tag{7}$$

and

$$\sin\phi_0 = -\Delta_x/P, \quad \cos\phi_0 = \Delta_y/P. \tag{8}$$

In the strict thin prism model P is a positive and monotonically increasing function of radial distance. Accordingly, Equation 7 for P and Equation 8 for ϕ_0 are entirely unambiguous. Later, we shall have occasion to relax the thin prism model by allowing P to assume both positive and negative values. To avoid ambiguities of sign under such circumstances, we shall invoke bilateral symmetry to restrict ϕ_0 to the range $0 \leqq \phi_0 \leqq 180°$. This means that $\sin\phi_0$ can assume only positive values and, hence, that the sign of P must always be taken opposite that of Δ_x.

The character of thin prism distortion is illustrated in Figure 2. Here, we have analytically projected a grid with 20 mm. divisions through a thin prism ($\mu = \sqrt{2}$, $\epsilon = 10'$) onto a hypothetical camera of 600 mm. focal length and 17°×17° field. The azimuth of the prism has been taken as $\phi_0 = 0°$, and the true elements of orientation have been specified as $\alpha = 0$, $\omega = 0$, $\kappa = 0$, $x_p = y_p = 0$, $c = 600$ mm. Because $\phi_0 = 0$, Equation 6 reduces to $\Delta_x = 0$, $\Delta_y = P$, and the distortion in Figure 2 is entirely in the y direction. The results of Figure 1 constitute an analytical parallel to the experimental results of Washer (1957b) in which a target array was photographed both with and without a thin prism in front of the lens. In the present case, however, the object points are at infinity, whereas in Washer's case they are at a sensibly finite distance (namely, a distance of approximately three

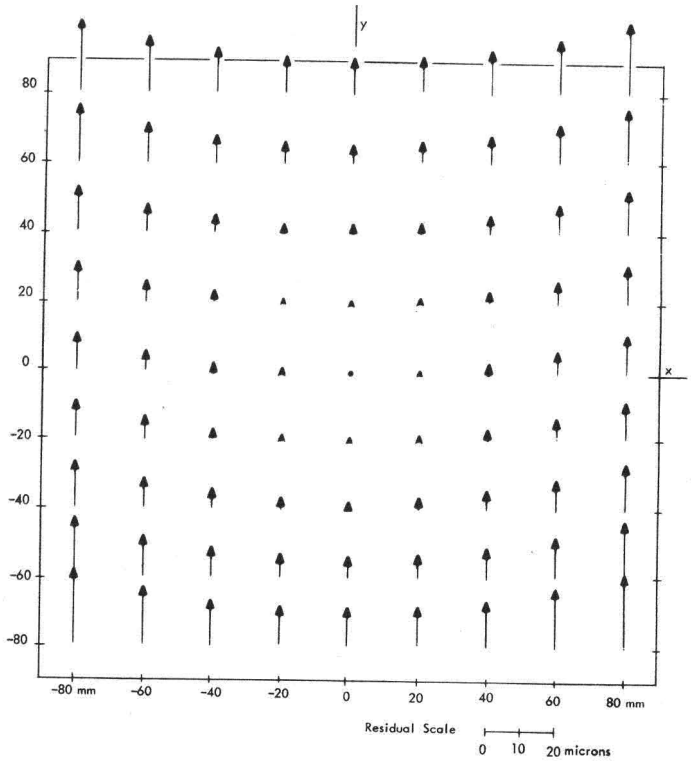

FIG. 2. Residual vectors of thin prism distortion when true elements of orientation are enforced ($\mu=\sqrt{2}$, $\epsilon=10'$, $\phi=0$, $c=600$ mm.); mean error $=7.7\mu$.

focal lengths from lens which leads to a 2× reduction of the target array). We believe that this significant difference in object space distances accounts for the partial discrepancies between Washer's results and ours.

PROPAGATION OF THIN PRISM DISTORTION THROUGH LEAST SQUARES PROJECTIVE TRANSFORMATION

During the course of the past decade we have had the opportunity to study the residual vectors from scores of stellar plates, each taken explicitly for the calibration of symmetric radial distortion and each containing from 100 to 200 fairly uniformly distributed images. In those cases where decentering distortion was sufficiently large to be obvious from visual inspection of the residuals, the general nature of the systematic pattern bore little resemblance to that of Figure 2, due allowance being made for a rotation in ϕ_0. This is not surprising, for in a least squares stellar calibration the elements of orientation will naturally adjust in such a manner as to minimize the quadratic form of the residuals. Therefore, the calibrated elements of orientation will compensate in part for the effects of decentering distortion, and the basic pattern of decentering residuals will be altered by the compensative process.

In order to gain insight into the precise nature of the compensation resulting from a least squares projective transformation, we subjected the plate coordinates of the distorted grid of Figure 2 to a least squares adjustment under the assumption that the grid coordinates in object space were perfectly known. The resulting residual vectors are plotted in Figure 3 (the pair of curves plotted in the figure are for future reference). The 'calibrated' elements of orientation turned out to be $\alpha=0°$, $\omega=0°.0255$, $\kappa=0°$, $x_p=0$, $y_p=0.260$ mm., $c=600.000$ mm. This demonstrates that the basic mechanism afforded by elements of orientation for compensation consists of:

a. A shift of the principal point away from the edge of the prism,

b. A tilt of the camera axis away from the edge of the prism (α corresponds to x tilt and ω to y tilt),

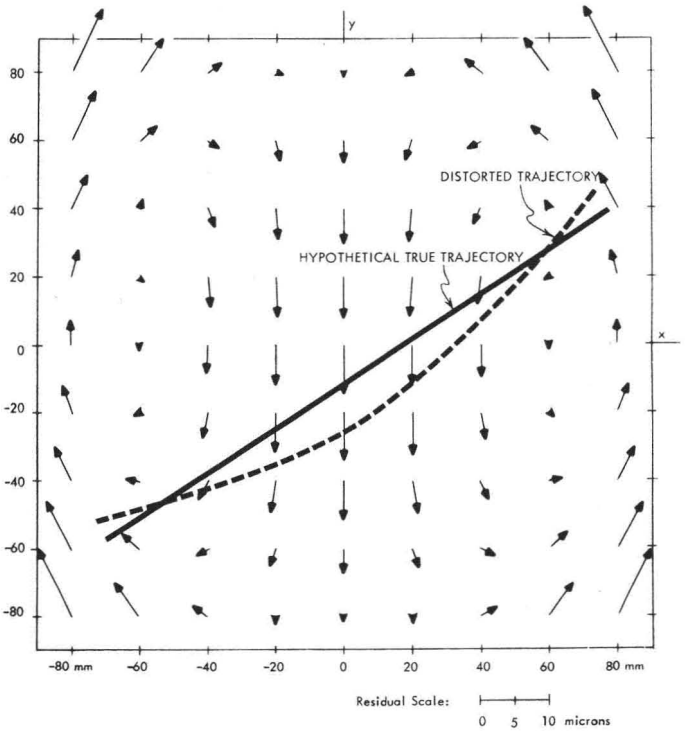

FIG. 3. Residual vectors of thin prism distortion when elements of orientation are obtained from least squares adjustment (same thin prism parameters as in Figure 2); mean error = 3.6μ.

It is noteworthy that the principal distance does not enter into the compensative process and that the compensative translation of the plate and tilt of the camera are both confined to the principal section of the prism. In comparing Figures 2 and 3 one should note that the scales of the residual vectors differ by a factor of two. The rms error of the raw residuals of Figure 2 is 7.7 μ, whereas that of the residuals of Figure 3 is 3.6 μ, a more than two-fold improvement. The residual vectors after the least squares projective transformation are no longer strictly unidirectional as in Figure 2 but have sizeable components in both x and y. As we shall illustrate presently, the general pattern of the residual vectors of Figure 3 correlates well with the observed pattern of the systematic components of residual vectors resulting from stellar calibrations of symmetric radial distortion.

PROJECTIVE COMPENSATION OF THIN PRISM DISTORTION FOR WIDE ANGLE CAMERAS

With narrow projective bundles (as in Figures 2 and 3) a small shift of the principal point is very nearly the projective equivalent of a small tilt of the camera axis. This near equivalence or translation and rotation does not hold for wide projective bundles. In order to determine the nature of the compensative process for wide projective bundles, we repeated the computations leading to Figures 2 and 3 for a lens of 115 mm. focal length and 76°×76° angular field. The prism angle was changed from 10′ to 2′ so that the general magnitude of the distortion would be unaltered (as is clear from Equation 5, the effects of thin prism distortion vary as a direct product of prism angle and focal length). Because the residual patterns before and after projective compensation turned out to be practically identical with those of Figures 2 and 3 respectively, they are not reproduced here. The only essential change in the over-all results was that the principal point underwent essentially no adjustment in the case of the wide projective bundle (the value $y_p = 0.1$ μ was obtained); all compensation resulted from a tilt of the camera axis away from the edge of the prism. This corroborates Washer's (1957b) observation that an appropriate tilt of the camera can offset to an appreciable extent the effects of the asymmetric radial component of thin prism distortion.

Analytical Expressions for Projective Compensation

From the fact that compensative translation and tilt are confined to the plane of the principal section of the prism it can be demonstrated analytically that the equations for thin prism residuals resulting from projective compensation (as in Figure 3) are of the following form:

$$\begin{aligned}\Delta_x &= -(P + b - c\gamma)\sin\phi_0 \\ &\quad - \frac{\gamma}{c} r^2 \cos\phi \sin(\phi - \phi_0) \\ \Delta_y &= (P + b - c\gamma)\cos\phi_0 \\ &\quad - \frac{\gamma}{c} r^2 \sin\phi \cos(\phi - \phi_0) \end{aligned} \tag{9}$$

in which b (same units as c) and γ (radians) denote the magnitudes of the compensative translation and tilt. The corresponding expressions in terms of radial and tangential components are

$$\Delta_r = \left(P + b - c\gamma - \frac{\gamma}{c} r^2\right)\sin(\phi - \phi_0) \tag{10a}$$

$$\Delta_t = (P + b - c\gamma)\cos(\phi - \phi_0). \tag{10b}$$

These relations explain fully the nature of projective compensation. In particular, they clarify the relative roles of translation and tilt. As we have seen, the translation b is essentially unexercised in the compensative process for wide angle cameras. On the other hand, it performs an important function in the compensative process for narrow angle cameras, for here tilt compensation by itself is relatively ineffective. By largely, though not quite completely, counteracting the effect of tilt, the translation b permits the application of a tilt which would otherwise be excessively large. As a result, the term $(\gamma/c)r^2$ can become sufficiently large to be effective in the above expression for Δ_r and yet not lead to overcompensation in the expression for Δ_t.

Equation 10b shows that for $\phi = \phi_0$ the value of Δ_t becomes equal to $b - c\gamma$ at $x = y = 0$ (here, $P = 0$). This demonstrates that tangential distortion is not zero at the origin after compensation. Moreover, since $P + b - c\gamma$ passes through zero at a sufficiently large radial distance, it follows that tangential distortion can assume both positive and negative values across the format. The shape of the tangential profile is unaltered by the compensative process, which does nothing more than to translate the profile by the amount $b - c\gamma$, thereby producing a positive and negative balance of the profile across the format.

By contrast the compensative process for the radial component involves not only the translation $b - c\gamma$, but also the second order term $-(\gamma/c)r^2$, which serves to counteract much of the effect of the leading term of the expansion for P given by Equation 5.

This explains why projective compensation is appreciably more effective in reducing the radial component of thin prism distortion than in reducing the tangential component. We find, for example, that prior to projective compensation the rms values of the radial and tangential components in Figure 2 are both equal to 5.4 μ, whereas after projective compensation (Figure 3) they become 2.5 and 4.2 μ respectively. Perhaps the effectiveness of projective compensation explains why the radial effects of decentering have received relatively little recognition in the literature.

Another possible reason is that the nature of the radial component is such that it has no effect on the angle subtended by pairs of radially symmetric points. This would render impossible the detection of the radial component in those procedures of lens calibration which depend intrinsically on the determination of the relative radial displacements of opposing pairs of targets symmetrically arrayed across the diagonals of the plate. Only when the measurements are made relative to a central target imaged precisely at the principal point of autocollimation (as in Washer's investigation) can the existence of the radial component be detected and separated with certainty from possible effects of camera tilt. Indeed, it is to avoid such exacting alignment of the camera that some methods for the calibration of radial distortion deliberately avoid referring the measurements to a central target and thereby implicitly forego the possibility of measuring asymmetric radial distortion.

Conrady's Model for Decentering Distortion

In our discussions above we have scrupulously avoided considering thin prism distortion to be equivalent to decentering distortion. This was done in anticipation of the present section in which we shall review a set of rigorous results derived by Conrady (1919) in an elegant but little known paper. Except for Conrady, all of the references cited thus far have uncritically adopted the thin prism model as accounting for decentering distortion. It seems that Conrady's paper is not well known, for in all the literature we have reviewed, it is cited only by Livingston (1951)

and there only in oblique justification for the thin prism model as it pertains to tangential distortion. As we shall see, Conrady's model is in agreement with the thin prism model regarding the tangential component of decentering distortion but is substantially at variance with the thin prism model regarding the radial component. Conrady's results are based on analytical ray tracing through a decentered lens and are therefore exact through the order of the terms carried. They consider not only the effects of decentering on distortion but also its effects on the other aberrations as well. In particular, Conrady shows that decentering has the following major primary effects:

1. It introduces a coma that (like normal coma) varies with the square of aperture and (unlike normal coma) is uniform over the field both in magnitude and in direction;
2. It introduces an astigmatism characterized by image patches in the form of ellipses varying in length, eccentricity and orientation in different parts of the field;
3. It introduces a distortion having radial and tangential components given by (in our notation)

$$\Delta_r = 3P \sin(\phi - \phi_0)$$
$$\Delta_t = P \cos(\phi - \phi_0) \qquad (11)$$

the origin on the plate being taken at the principal point of autocollimation.

It should be noted that Conrady's $p_3 V^2$ corresponds to our P and that his angle χ corresponds to our angle of $90-(\phi-\phi_0)$. Conrady demonstrates that the above properties hold for a system having any number of decentered surfaces.

The first and second consequences of decentering affect the shape of the image patch but not the position of its center relative to other images; moreover, in reasonably well centered lenses these effects are likely to be almost imperceptibly small in relation to the classical aberrations. The third effect is thus the only one of possible metric consequence. Comparing Conrady's expressions for Δ_r, Δ_t with the thin prism Expressions 2, we find that the two models agree for Δ_t but differ by a factor of three for Δ_r. It follows that, as it stands, the thin prism model only partially accounts for the effects of decentering distortion and would appear to be substantially inadequate with regard to the radial component. As we shall presently see, this apparent discrepancy is of no projective consequence insofar as first order effects are concerned.

In Figure 4 we have plotted residual vectors for decentering distortion according to Conrady's model. Here, we have adopted the same tangential profile, the same value of ϕ_0 and the same elements of orientation as in Figure 2. We see from Figure 4 that the primary residual vectors of decentering distortion are not unidirectional as are the primary residual vectors thin prism distortion (note that the scales of the residual vectors in Figures 2 and 4 differ by a factor of two). The x, y components of decentering distortion are given by the following analytical expressions:

$$\Delta_x = -P\left[\left(1+2\frac{x^2}{r^2}\right)\sin\phi_0 - 2\frac{xy}{r^2}\cos\phi_0\right]$$
$$\Delta_y = -P\left[2\frac{xy}{r^2}\sin\phi_0 - \left(1+2\frac{y^2}{r^2}\right)\cos\phi_0\right]. \qquad (12)$$

These expressions are appreciably more involved than their counterparts for thin prism distortion (Equation 6).

Propagation of Decentering Distortion through Least Squares Projective Transformation

As we did for the thin prism distortion of Figure 2, we subjected the primary decentering distortion of Figure 4 to a least squares projective transformation. The resulting transformed pattern turned out to be identical in every respect with Figure 3 and so is not separately presented. From this, we may conjecture that the thin prism model is projectively equivalent to Conrady's model and that the thin prism model provides a suitable model for decentering distortion if it is modified to embrace a suitable translation of the plate and tilt of the camera. The elements of orientation resulting from the least squares projective transformation of Figure 4 are: $\alpha=0$, $\omega=0.°1431$, $\kappa=0$, $x_p=0$, $y_p=1.491$ mm., $c=600.000$ mm. The elements undergoing adjustment (ω and y_p) are in this case several times larger than the corresponding values for thin prism distortion, a result to be expected from the threefold larger radial component of decentering distortion.

We shall now examine the mechanism leading to the apparent projective equivalence of thin prism distortion and decentering distortion. The radial and tangential components of decentering distortion resulting from the application to Equation 11 of a translation b' and a tilt γ' can be shown to be given by

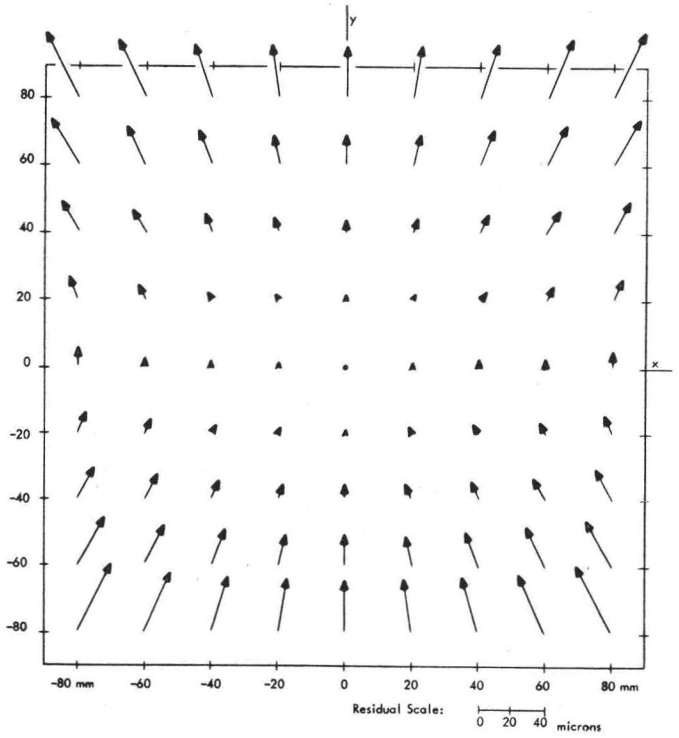

FIG. 4. Residual pattern caused by decentering distortion according to Conrady's model for lens having same tangential profile as thin prism of Figure 2. (Note that the scale of the residual vectors in this figure differs by a factor of two from that of Figure 2.)

$$\Delta_r = \left(3P + b' - c\gamma' - \frac{\gamma'}{c} r^2\right) \sin(\phi - \phi_0)$$
$$\Delta_t = (P + b' - c\gamma') \cos(\phi - \phi_0). \qquad (13)$$

According to Equation 5 the profile function can be expressed to the first order in r^2 as $P \approx J_1 r^2$. If this substitution is made in Equations 10 and 13 and if the radial and tangential components of transformed thin prism distortion are equated to the corresponding transformed components of decentering distortion, the following results are obtained upon reduction

$$b' = b + 2J_1 c^2$$
$$\gamma' = \gamma + 2J_1 c.$$

These relations between the two sets of compensative motions are independent of r, a result of pivotal importance stemming directly from the expression of P as equivalent to $J_1 r^2$. This means that as long as P is of the form $J_1 r^2$, the two models are projectively equivalent, for an appropriate translation and tilt can be found that will transform the one pattern of distortion into the other for all values of r. Indeed, it is to be noted that the first order projective equivalence of the two models is not dependent on the specific ratio of three between their respective radial components, but would hold as well for any ratio, say k, in which case the factors of two on the right hand sides of the above equations would be replaced by k-1.

We shall shortly find that in certain instances at least one higher order term in r^2 may be required in the profile function. When higher order terms are significant, the strict projective equivalence of thin prism and decentering distortion no longer holds. In view of this and in view of the special auxiliary translation and tilt required to render the thin prism distortion equivalent to decentering distortion (a process, we would emphasize, that is possible only when higher order effects are insignificant), we suggest that the thin prism model be abandoned entirely as a model for decentering distortion. Conrady's model as expressed either by Equations 11 or 12 provides the more suitable model for decentering distortion the validity of which in no way depends on artificial compensative motions of the plate and camera.

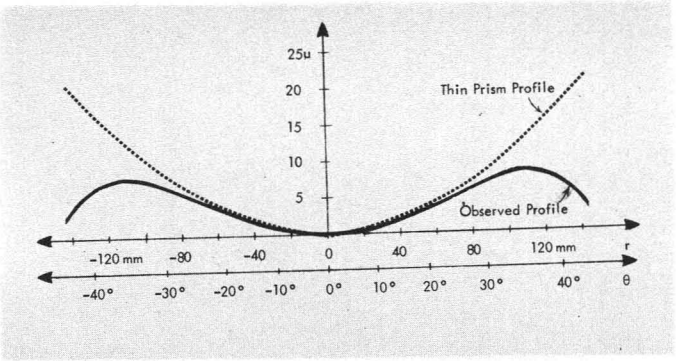

FIG. 5. Average Profile function of tangential distortion obtained by Livingston from measurements of 33 Metrogon lenses as compared with most nearly equivalent thin prism profile.

HIGHER ORDER EFFECTS OF DECENTERING

As we have already noted, Livingston's (1951) results for wide angle lenses (Metrogons subtending $74°\times74°$ fields) are not generally in strict accord with the thin prism model, for the typical tangential profile P (Figure 5) found by Livingston is not monotonic as required by the thin prism model but rather reverses its direction towards the edge of the field. This observed reversal of tangential distortion cannot be explained by errors in camera set up as would have been the case had such reversal been observed in the asymmetric radial profile; the tangential reversal is clearly real and not a consequence of experimental procedure. It is noteworthy that Livingston's experimental results demonstrate the validity of the cosine variation of tangential distortion, reversal and all. Although reversal cannot be explained by the thin prism model, presumably it could by the higher order terms of Conrady's model. Unfortunately, Conrady does not develop these terms and, in lieu of supplementary analytical results, we must resort to conjecture concerning the nature of the higher order effects of decentering. All available evidence suggests that higher order effects can adequately be accounted for simply by adding powers of r^2 to the profile function which then assumes the form:

$$P = J_1r^2 + J_2r^4 + J_3r^6 + \cdots \qquad (14)$$

As with higher order thin prism distortion, the exact profile function for decentering distortion will, we believe, ultimately be found to be weakly dependent on azimuth ϕ. Be this as it may, experience to date indicates that Conrady's model given by Equation 11 or 12, as modified by the incorporation of the expanded profile Function 14, provides a working model for decentering distortion that is sufficient for all practical needs.

Inasmuch as a decentered lens partially conforms to the thin prism model, it is clear that, as a secondary effect, decentering will cause the image patches to be broken down into minute spectra. In the strict sense, this means that the coefficients of the profile functions J_1, J_2, . . . are color dependent. However, chromatic effects of decentering distortion are likely to assume practical significance only for objectives of very long focal length such as are used for astronomical observations.

RELATIONSHIP BETWEEN PRINCIPAL POINT OF PHOTOGRAMMETRY AND PRINCIPAL POINT OF AUTOCOLLIMATION.

In the projective equations relating image and object spaces, the fundamental point of reference on the plate is the principal point of photogrammetry (x_p, y_p). In the analytical process of calibration this point is recovered relative to the plate center as defined by a system of fiducial marks. However, in our discussions of decentering distortion the natural origin of the plate coordinate system becomes the principal point of autocollimation $(x_{pa'}, y_{pa})$. Inasmuch as the displacement of the two principal points must lie along the radius vector of angle $90°+\phi_0$, the two points are interrelated by

$$\begin{aligned} x_{pa} &= x_p + \rho \sin \phi_0 \\ y_{pa} &= y_p + \rho \cos \phi_0 \end{aligned} \qquad (15)$$

where ρ denotes the distance between the two points. In the thin prism model ρ is given by

$$\rho = c(\mu - 1)\epsilon$$

and ϵ, the prism angle, can in turn be computed from the leading coefficient J_1 of the tangential profile by means of

$$\epsilon = \frac{2c\mu J_1}{(\mu - 1)(\mu + 1)}.$$

In Conrady's model the displacement in the principal section is three times greater than in the thin prism model and the appropriate expression for ρ accordingly becomes

$$\rho = 3c(\mu - 1)\epsilon.$$

Although, as we have already noted, the value of μ may be regarded as arbitrary insofar as the tangential profile is concerned, this option no longer holds when the separation of the principal points becomes a consideration, for the value of ρ will clearly vary with each choice of μ. It follows that either ρ or μ must be viewed as constituting an independent parameter when an attempt is made in the reduction to recover the principal point of autocollimation relative to the principal point of photogrammetry. By letting ρ rather than μ be the independent parameter, one makes no specific commitment to either the thin prism model or Conrady's model and accordingly one obtains a model valid for a combination of decentered optics and prismatic filters.

To accomplish the calibration of ρ, one need merely replace x and y as considered in foregoing development by the expressions

$$x - x_p - \rho \sin \phi_0,$$
$$y - y_p - \rho \cos \phi_0$$

in which ρ now constitutes an additional parameter to be recovered in the calibration (at this point we should again note that the coordinates of the principal point x_p, y_p are invariably recovered in a definitive calibration and hence do not constitute new parameters arising from a consideration of decentering). When decentering is small, the analytical recovery of ρ is likely to be marginal because the variation in the partial derivatives of the x and y coordinates with respect to ρ is very slight throughout the format, a consequence of the fact that the variation in these derivatives depends primarily on the ordinarily small magnitudes of the coefficients of decentering distortion J_1, J_2, $\cdots$ and coefficients of symmetric radial distortion K_1, K_2, $\cdots$ (here it should be noted that the principal point of autocollimation serves also as the natural origin for computing the radial distances entering the expressions for symmetric radial distortion).

In most calibrations attempts to recover ρ to meaningful precision are likely to prove futile, for the coordinates x_p, y_p can generally strike a practical and effective compromise that renders ρ projectively superfluous. On the other hand, with cameras of fairly long focal length (on the order of several meters), the value of ρ may amount to several millimeters for moderate decentering. Here, the separation between the principal points can conceivably assume projective significance, particularly when symmetric radial distortion is also large. In view of this, there may be merit in carrying ρ provisionally through certain reductions as an adjustable parameter, subsequently to be dropped in the event that its inclusion fails according to an F-test to reduce significantly the quadratic form of the residuals.

Precise Analytical Calibration of Decentering Distortion

Decentering distortion can be calibrated analytically in the same manner as has been used successfully for years in the case of symmetric radial distortion (Brown, 1956), namely by incorporating the mathematical model for decentering distortion into the original projective equations generated by the plate measurements and by solving the resulting system of normal equations for the decentering parameters in addition to the other parameters normally carried (elements of orientation, coefficients of symmetric radial distortion, parameters of atmospheric refraction, etc.). Inasmuch as the expressions for Δ_x, Δ_y are nonlinear in ϕ_0, the determination of a suitable initial approximation for ϕ_0 presents a problem. Even when a suitable approximation for ϕ_0 is available, it becomes necessary to assign a discrete (nonzero) initial approximation to J_1 in order to prevent the linearized coefficients of the correction to the approximation to ϕ_0 from being zero in all of the linearized observational equations. One way around this problem involves the exercise of successively relaxed a priori constraints as discussed in Brown (1964). However, a far more efficient and hitherto unpublished approach is employed in our current version of the advanced plate reduction. It involves the introduction of the new parameters P_1, P_2, P_3, $\cdots$ defined by

$$\begin{aligned} P_1 &= -J_1 \sin \phi_0 \\ P_2 &= J_1 \cos \phi_0 \\ P_3 &= J_2/J_1 \\ P_4 &= J_3/J_1 \\ &\vdots \end{aligned}$$

which recasts the extended expressions for Conrady's model into the form

$$\Delta_x = [P_1(r^2+2x^2)+2P_2xy][1+P_3r^2+P_4r^4+\cdots]$$
$$\Delta_y = [2P_1\,xy+P_2(r^2+2y^2)][1+P_3r^2+P_4r^4+\cdots].$$

If the higher order coefficients J_2, J_3 were zero, the above expressions for Δ_x and Δ_y would be reduced to linear functions of P_1 and P_2, and the initial approximations for these parameters could be taken as zero. For the more general case where higher order coefficients are to be considered, it suffices to adopt zero values for the initial approximations of all the P's, the only precaution being that arbitrary, but large, a priori variances be assigned to P_3, P_4, $\cdots$ to counteract (in the initial adjustment) the indeterminacy otherwise resulting from the zero initial approximations to P_1 and P_2. In subsequent iterations of the adjustment, the improved approximations to P_1 and P_2 become discrete, thus rendering the solution for P_3, P_4, $\cdots$ determinate.

We shall not go further into the details of the extension of the plate reduction to embrace the calibration of decentering distortion, for the computational mechanics of the procedure are fully covered in Brown (1964). Rather, we would point out that when parameters of decentering distortion are incorporated into the adjustment, the covariance matrix of the adjusted values of these parameters is contained in the inverse of the coefficient matrix of the normal equations. This means that the accuracy of the calibration can readily be computed for any specified points on the plate. In stellar calibrations involving on the order of 200 well distributed stars, the error in calibrated decentering distortion can generally be suppressed to one micron or less at the extreme corners of the format and to an rms value over the entire plate of about 0.4 microns.

Experimental Results

To this point all results have been based solely on analytical considerations coupled with supporting numerical simulations. In order to test the theoretical results we resorted to a special physical experiment. In cooperation with Space Systems Laboratories of Melbourne, Florida, we obtained stellar plates from a pair of Pth 60 Phototheodolites manufactured by SSL. The cameras have focal lengths of nominally 600 mm., effective apertures of about 200 mm., and angular fields of $17°\times17°$. They are designed to use 6-mm. thick plates of dimensions 190×215 mm. One of the cameras (SSL 001) was known by inspection on an optical turntable to be out of alignment to the extent that small further physical adjustment would have been distinctly worthwhile. The second camera (SSL 002) was considered by optical technicians to be aligned to the practical limit of their art and hence was deemed not to be subject to further meaningful physical improvement.

The stellar exposures were made simultaneously for both cameras, the cameras being side by side, and were of a common zenithal field. Kodak Microflat glass plates coated with 103 F emulsion were employed. The plates were photographically processed together and were measured on a calibrated Mann comparator by the same operator on different days. A total of 155 well-distributed images were measured on each plate, a pair of settings being made on each image. The plate measurements were subjected to the advanced plate reduction developed in Brown (1964), the appropriate parameters being carried for symmetric radial distortion but none being carried for decentering distortion. No allowance was made for star catalog error, even though the General Catalog was employed (typical GC error is equivalent to about 2 microns on the plate of 600 mm. camera). This was deliberate and was done to prevent any possibility that the adjustment of stellar positions might partially compensate for locally significant systematic effects. The x, y least squares residuals therefore reflect not only random error in the plate coordinates, but also random error in the stellar coordinates as well as systematic error (such as decentering error) not fully accountable by the mathematical model of the reduction. The residual vectors for SSL 001 and 002 are plotted in Figures 6 and 7 respectively.

Very definite systematic tendencies of the residual vectors are obvious from a visual inspection of Figure 6. When due allowance is made for the random component of the residual vectors, we see that the general systematic pattern of Figure 6 is in excellent correspondence with that of Figure 3 as rotated by about 70°. This correspondence provides solid experimental confirmation of our theoretical results. It is noteworthy that even though pronounced systematic effects are evident in Figure 6, the rms error of the residual vectors is only 3.9 microns, a result demonstrating the effectiveness of projective compensation.

The systematic effects so pronounced for SSL 001 are absent from 002 (Figure 7). This does not necessarily mean that decentering distortion is insignificant for 002, but rather that it is sufficiently small relative to the random error to elude casual visual detection. In

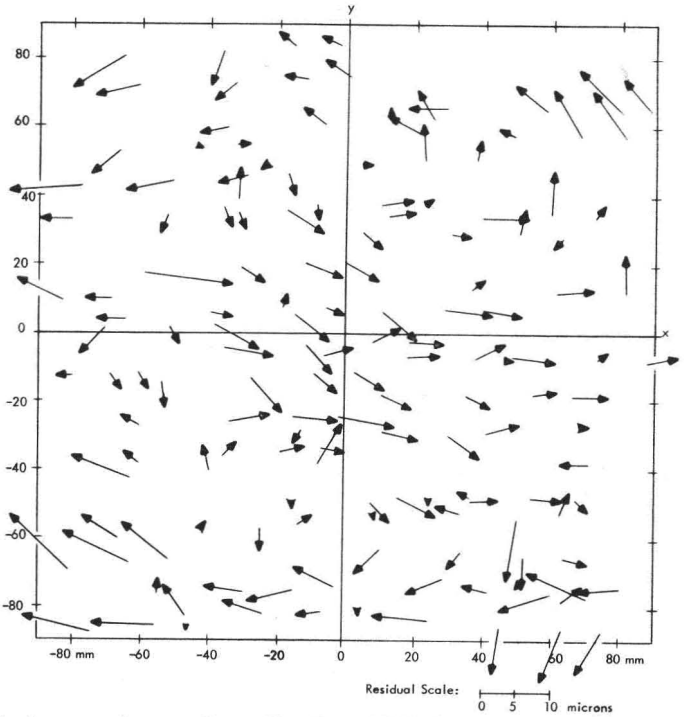

FIG. 6. Residual vectors from stellar calibration of SSL Camera 001 as obtained from least squares solution for elements of orientation (no parameters carried for decentering distortion); mean error = 3.9μ.

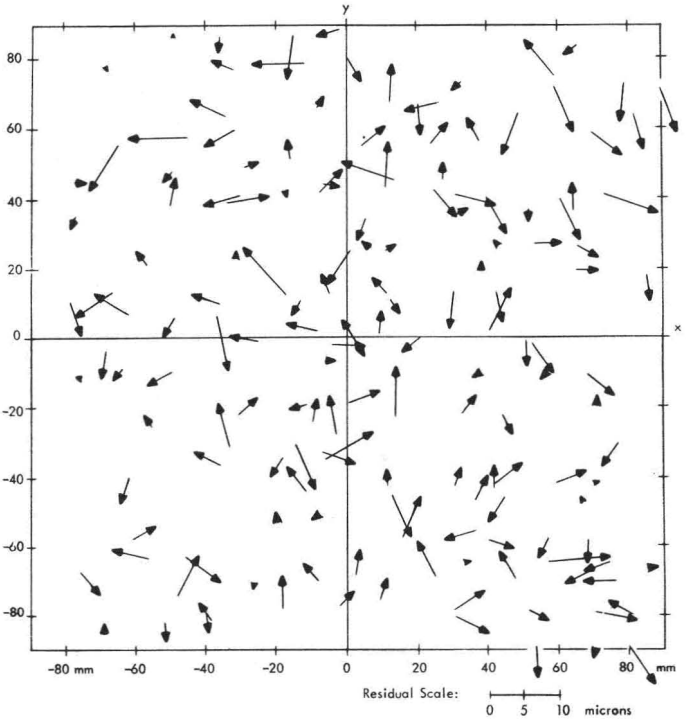

FIG. 7. Residual vectors from stellar calibration of SSL Camera 002 as obtained from least squares solution for elements of orientation (no parameters carried for decentering distortion); mean error = 3.4μ.

TABLE 1. MEAN ERRORS RESULTING FROM VARIOUS ADJUSTMENTS

Camera	*Number of Control Points*	*Case I*	*Case II*	*Case III*	
		Mean Error of Plate Coord. Residuals	*Mean Error of Plate Coord. Residuals*	*Mean Error of Plate Coord. Residuals*	*Mean Error of Stellar Coord. Residuals*
SSL 001	155	3.9μ	2.5μ	2.1μ	0.″27
SSL 002	155	3.4μ	3.1μ	2.8μ	0.″34

Case I. Star catalogue error and decentering distortion are not explicitly considered in the adjustment (residuals plotted in Figures 6 and 7).

Case II. Decentering distortion, but not star catalogue error, is rigorously treated in the adjustment.

Case III. Star catalogue error and decentering distortion are both rigorously treated in the adjustment (plate coordinate residuals for Camera 001 are plotted in Figure 8).

view of typical plate measuring accuracies of 2 to 3 microns, it is altogether conceivable that even after projective compensation, residual decentering distortion might amount to as much as 3 to 4 microns in some parts of the field and have an rms error of as much as 2 microns. It is therefore clear that a need exists for a method of evaluating possible decentering distortion that is more powerful and less subjective than visual inspection of least squares residuals. As indicated earlier, an objective solution to this problem consists of recovering the parameters of decentering distortion within the plate reduction itself.

RESULTS OF STELLAR CALIBRATION OF DECENTERING DISTORTION

With the plate reduction extended to incorporate parameters for decentering distortions, we repeated the stellar reductions for SSL Cameras 001 and 002. Results of three different reductions of varying levels of refinement are summarized for each camera in Table 1 and the final residual vectors for 001

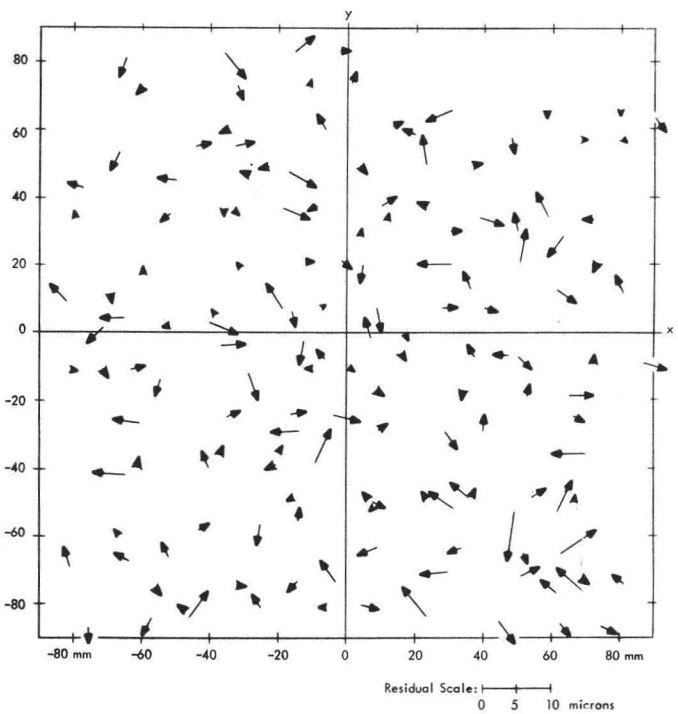

FIG. 8. Residual vectors from stellar calibration of SSL Camera No. 001 as obtained from Advanced Plate Reduction considering decentering distortion and random error in star catalogue (same original data as in Figure 6); mean error = 2.1μ.

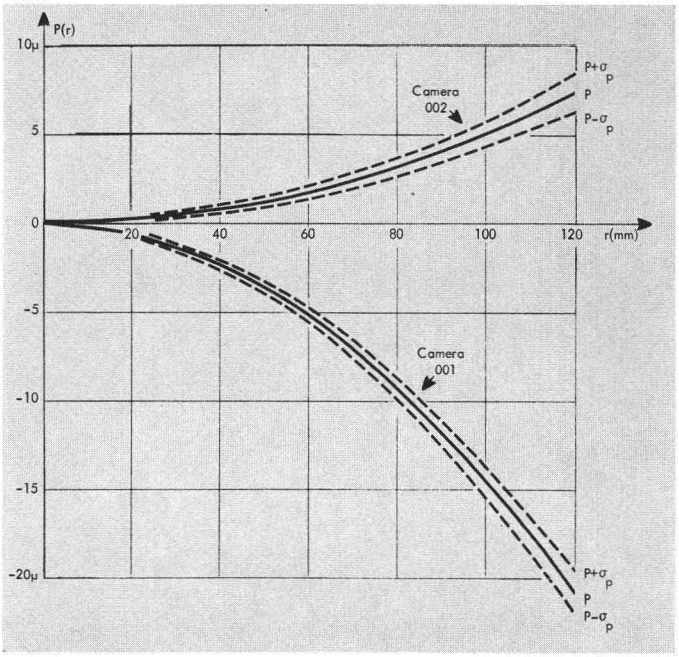

FIG. 9. Profile functions and associated one sigma confidence limits of decentering distortion resulting from stellar calibrations of SSL Cameras 001 and 002 by means of the Advanced Plate Reduction.

are plotted in Figure 8. The calibrated profile functions $P(r)$ for both cameras are presented together with their one sigma confidence limits in Figure 9. We see from Figure 9 that decentering distortion for 001 is nearly three times as great as for 002 and amounts to about 15 microns at a radial distance of 100 mm. The one sigma error bounds of the calibrated tangential profiles reach the level of one micron only in the corners of the format. It follows that decentering distortion is amenable to very precise calibration.

Although the calibrated profile function for 002 grows to 5 microns at 100 mm., it should be kept in mind that this is representative of the profile function without the benefit of projective compensation. When such compensation is operative (as in Figure 7), the maximum value of the profile for 002 is reduced to about 3 microns and its rms value is on the order of 1.5 microns. This provides a good illustration of how decentering distortion can be significant (by ballistic camera standards) and yet not be detectable from visual examination of residuals.

In comparing the residual vectors of Figures 6 and 8 we note that the extended plate reduction has been completely successful in removing the systematic components of the residuals in Figure 6. The randomness of the residual vectors achieved in Figure 8 is entirely satisfactory. The mean error of 2.1 microns achieved in the extended reduction is only slightly more than half as great as the mean error of 3.9 microns resulting when decentering distortion was not explicitly taken into account. The two parameters ϕ_0 and J_1 were found to be sufficient for the calibration of both cameras; the coefficient J_2 was carried initially but was dropped for failing to lead to a statistically significant reduction of the quadratic form of the residuals. The calibrated values of the decentering parameters are (for P and r in mm.) given in Table 2.

TABLE 2. CALIBRATED VALUES OF DECENTERING PARAMETERS.

Camera SSL 001	Camera SSL 002
$\phi_0 = 71°.9 \pm 3°.1$	$\phi_0 = 6°.6 \pm 10°.6$
$J_1 = (-1.456 \pm .075) \times 10^{-6}$	$J_1 = (0.502 \pm .089) \times 10^{-6}$

The appreciably greater mean error of ϕ_0 for 002 is attributable to the fact that the decentering distortion of 002 is appreciably smaller than that of 001. It should be appreciated that if there were no decentering distortion, ϕ_0 would be indeterminate for there would then be no axis of maximum tangential distortion. Hence, the greater the decentering distortion, the more sharply ϕ_0 is defined.

Inasmuch as random errors in the cataloged stellar positions were rigorously taken into account in the final adjustment, residuals were also obtained for stellar right ascensions and declinations. Each star was individually weighted according to the reciprocal of its updated variance as computed from appropriate entries in the catalog. It will be noted that the rms error of the stellar residuals for Camera 001 is only 0.″27 which corresponds to 0.9 μ on the plate. This relatively low value reflects the fact that the particular star field employed (Cygnus) is especially well determined in the General Catalog (two thirds of the 42 different stars carried had updated mean errors of less than 0.″40 and only 4 had mean errors in excess of 0.″60).

We consider that our combined theoretical and experimental results (including subsequent calibrations not reported here) demonstrate conclusively the feasibility of the precise analytical calibration of decentering distortion. In sections to follow we shall review some of the metric consequences of uncompensated decentering distortion.

Effects of Decentering Distortion on Geodetic Flash Triangulation

Since the first demonstration of the feasibility of employing ballistic camera observations for precise recovery of geodetic positions (Brown, 1958, 1959), full-scale global programs have been or shortly will be inaugurated (ANNA, GEOS, PAGEOS) to exploit this powerful geodetic tool. We shall consider here how decentering distortion, if not explicitly taken into account in the reduction, can be expected to lead to gross biases in recovered geodetic heights in spite of all efforts to obtain improved accuracies through the exploitation of seemingly overwhelming redundancy of observations and plates.

The mechanism of the biasing process is best explained through a reconsideration of the residual effects of decentering distortion following least squares projective compensation as illustrated in Figure 3. The heavy, solid line partially crossing Figure 3 represents the trace of a hypothetical trajectory as it would appear if there were no decentering distortion. The broken curve represents the displacement of the trace attributable to the residual decentering distortion of the figure (this displacement is magnified 2000 times, as are the residual vectors). We see that for the case under consideration, the effect of residual decentering distortion is to introduce a mean bias along the trace of about -5 microns, predominantly in the direction of the y-axis.

We should particularly note that with the exception of the far corners of the format, the effects of residual decentering distortion are largest near the center of the plate and moreover are of almost constant direction within this region. This means that no matter from what direction a reasonably well centered trace crosses the plate, the mean bias attributable to decentering will be of nearly the same direction and of nearly the same magnitude on plate-after-plate taken by a given camera.

Let us, for the moment, assume that the hypothetical camera giving rise to Figure 3 were on an alt-azimuth mount with the $+y$-axis pointing in the direction of increasing elevation angle and the $+x$-axis pointing in the direction of increasing azimuth. Then on plate after plate taken by the hypothetical camera, the mean bias of -5 microns or so would constitute a bias predominantly in a reconstructed elevation angles of the rays. If the camera had a 1000 mm. focal length, the mean bias in elevation angle would amount to about $-1''$ of arc; if 300 mm. focal length, it would amount to about $-3''$ of arc. The predominant effect of a more or less constant bias in the elevation angles of all of the rays converging on a given station would clearly be to introduce a bias into the recovered height of the station.

By contrast, if the various groups of rays from a moderate number of plates were well-balanced in azimuth about the station, the residual effects of decentering distortion in the elevation angle would largely average out in the recovery of the horizontal coordinates of the station. The effectiveness of this averaging process would hold equally well if the rays were affected by significant azimuthal decentering biases as, for example, would be the case if the axis of maximum decentering distortion in Figure 3 were rotated by 45°.

It follows, then, that what need concern us in a well-balanced resection is the mean component of residual decentering distortion in the direction of the elevation angle. If this component amounts to p microns for a camera

of focal length c microns, and if $\overline{R}$, $\overline{E}$ denote, the mean slant range and elevation angle of the rays from the station to the points observed, the bias β_h to be expected in the recovered height of the station is given roughly by

$$\beta_h \approx \frac{P}{c} \overline{R} \sec \overline{E}. \tag{16}$$

The derivation of this approximation depends on the assumption that unbiased coordinates of the flashes are independently available, thus reducing the geodetic problem to the limiting case of independent resections. It bears emphasizing that the above result would hold no matter how many plates were employed in the reduction for a given station; the bias in height attributable to uncompensated decentering distortion is not amenable to significant reduction through sheer exercise of redundancy.

We believe that residual decentering distortion provides the most likely explanation for the untoward discrepancies encountered in the recovery of heights of BC-4 camera stations employed on a test triangle as reported in Bulletin 24 of the U. S. Coast and Geodetic Survey (1965). This test triangle involved stations about 1500 km. apart in Maryland, Minnesota and Mississippi. BC-4 ballistic cameras equipped with synchronized shutters passively observed several passes of Echo 1. The horizontal coordinates recovered in a six-pass reduction for the two stations treated as unknown (Minnesota and Mississippi) were found to be in good agreement with the pre-existing first order survey, the discrepancies amounting to only a few meters, and being consistent with the combined standard errors of the two surveys. The discrepancies in the heights of the two unknown stations, on the other hand, amounted to about -20 to $+31$ meters respectively. These discrepancies compare unfavorably with the expected standard errors of 6.3 and 3.9 meters attributable to random errors of the photogrammetric measurements and with the standard errors of about 5 meters attributable to the astro-geodetic heights. If we take the mean distance of the rays to Echo to be $\overline{R} \approx 2.5 \times 10^6$ m., and the mean elevation angle of the rays to be $\overline{E} = 45°$, we find from Equation 16 that for cameras of 300 mm. focal length mean decentering biases in the direction of elevation angle of $p = -1.7$ microns and $p = 2.6$ microns, respectively, would suffice to explain the observed discrepancies in the heights of the stations under the assumption that the coordinates of the flashes were unbiased. This degree of residual decentering distortion at the center of the plate is altogether plausible (indeed likely) for cameras of high metric quality.

It should be noted that the ultimate effects of residual decentering distortion are accentuated by the particular reduction employed by the USCGS. The critical factor in this regard is that, following the least squares fit of a high order polynomial to the measured points on the trace, only a single ray on the fitted polynomial is retained for subsequent triangulation and this, being a central ray, is subject (as we have seen) to greater residual decentering distortion than any other possible choice with the exception of rays near the corners of the format. Although the smoothed plate coordinates corresponding to the central ray typically have standard deviations of only 0.2 μ, their associated systematic errors due to residual decentering distortion are, on the average, almost certain to range from five to fifteen times greater. Even so, the component of systematic error in elevation angle would have relatively small effect on the closures of triangulation and hence would largely elude detection from least squares residuals. In our view, it would have been better had USCGS evaluated the fitted polynomial at a pair of points having radial distances of 60 to 70 mm., for here residual decentering distortion approaches its minimum in those reductions employing stars over a substantial portion of the plate. Better still, of course, would have been the explicit consideration of decentering distortion within the plate reduction employed by USCGS.

An alternative, though a less satisfactory method of counteracting decentering distortion, consists of carrying in the reduction sets of carefully paired traces such that the two traces of a set cross the format in a similar manner but are recorded on plates differing nominally by 180° in roll angle. To the extent that decentering were independent of the forces of gravity acting on the lens, this process would allow appreciable cancellation of the systematic effects induced by decentering, for half of the rays would be biased positively and half negatively in elevation angle. The closures of the adjustment would, of course, be rendered appreciably larger by this process, for they would fully reflect the biases in the resecting rays. Clearly, this is a healthier and more desirable situation than one in which significant biases exist but are poorly reflected by the residuals.

The method of paired traces is readily applied to cameras such as the PC-1000 which can be rolled about the optical axis; in fact, it is almost an automatic by-product of the practice of rolling PC-1000's on each operation so that the flashing light trace crosses the plate on one or the other of the diagonals. This together with the fact that triangulation is not limited to central rays perhaps partially explains why it is that the recovered heights of a six station PC-1000 test network of dimensions comparable to those of the USCGS Maryland-Minnesota-Mississippi net have proven (Hadgigeorge, 1965) to be fully tenfold better in absolute agreement with astro-gravimetric heights than the corresponding BC-4 results reported in USCGS Bulletin 24.

Even when the decentering distortion of a given camera has been explicitly calibrated, we consider it prudent to employ the method of matched traces routinely as a safeguard against the possibility of significant accidental changes of decentering. Also, it is advisable to evaluate decentering at moderate zenith distances with the camera in both direct and plunged orientations in order to establish the influence, if any, of gravity on the results.

Effects of Decentering on Photogrammetric Extension of Control

In the past, many of the metric shortcomings of mapping cameras could be tolerated by virtue of the compensation provided by fairly dense networks of pre-established ground control. However, the establishment of a high level of control constitutes a major expense of the mapping operation in both time and money. For this reason coupled with advances in computer technology, the extension of mapping control by means of analytical aerotriangulation has aroused widespread interest. Recent breakthroughs (Brown, Davis, Johnson, 1964) have made feasible the uncompromisingly rigorous simultaneous adjustment of very large blocks of photography. However, the practical attainment of the full promise of analytical methods depends in great measure on the precise calibration of the camera; accuracies of calibration four to five times greater than those generally considered adequate in conventional mapping are needed if the fullest benefits of analytical methods are to be realized. This is because residual systematic errors propagate through analytical aerotriangulation in a most unfavorable manner. Thus, uncompensated decentering distortion as small as 2 to 3 microns has a rapid cumulative effect on the analytical reconstruction of a strip and assumes prominence relative to the effects of random errors within a few models. The admissible length of analytical extension between control is clearly a function of the geometric fidelity of the camera following application of all known corrections. Up to a certain point, the more comprehensive and more precise the calibration of the camera, the lower the requirements for absolute control in the photogrammetric net. As the application of analytical methods widens, we foresee the growth of increasingly stringent demands for improved accuracies of calibration of mapping cameras not only for symmetric radial distortion and elements of interior orientation, but also for decentering distortion.

Implications of Decentering Distortion on the Design of Metric Cameras

Because decentering distortion can be effectively removed through calibration, extremely precise centering need no longer be viewed as a stringent requirement for lenses to be employed in many photogrammetric applications, especially in applications to geodetic flash triangulation. Indeed, decentering can now be tolerated to the extent that it does not sensibly affect the quality of images. This means, in effect, that almost any well-regarded commercial lens of suitable focal length, aperture and angular field can be employed for metric observations, for it is image quality throughout the format that now becomes the overriding factor in the ultimate determination of metric potential. We have, for instance, been able to demonstrate that a specially modified commercial view camera employing a 480 mm. f/4.5 Schneider Xenar lens can produce stellar plates of superb quality over a cone angle of 20° and that, when properly reduced, can yield directional accuracies unsurpassed by any standard ballistic camera of comparable or shorter focal length. This demonstration points out that trifling technicalities and pedantic illusions have been permitted to obscure the physical essentials of the ballistic camera which, aside from focal length, aperture, and angular field, are merely twofold: (1) a high degree of short-term stability in any desired orientation (typically over a period of five to ten minutes) and (2) excellent image quality over the spectral range of interest. It is hoped that one consequence of this paper will be to counteract the sophistry that unfortunately has

come to be superimposed on optomechanical technology as it pertains to ballistic cameras.

Concluding Remarks

In our experience over the past decade with the full scale stellar calibration of over 50 different ballistic cameras for symmetric radial distortion, fully three quarters of the calibrations have yielded mean errors in the range 3.5 to 5.0 microns, a range incompatibly large relative to the 2 to 3 microns normally attributable to the combined effect of the plate measuring error corresponding to double settings, the random instability of the photographic emulsion, and all other sources of random error. Because of this it was usually deemed necessary in routine reductions following the calibration of radially symmetric distortion to resort to tedious piecewise procedures wherein two or three compact but overlapping groups of stars encircling different portions of long flashing light traces were individually reduced, the purpose being to allow the elements of orientation greater freedom for local compensation of unmodeled systematic errors. Only through such independent reduction of limited regions of the plate could least squares residuals yielding a mean error in the acceptable range of 2 to 3 microns be consistently obtained. In the light of our present findings we are now convinced that the uncomfortably large mean errors frequently encountered in past full scale stellar calibrations can largely be attributed to uncompensated decentering distortion. We are also convinced that the problem of decentering distortion has now been overcome, and that decentering distortion is fully as subject to precise analytical calibration as symmetric radial distortion. As we have indicated, this fact bears consequences of fundamental importance to geodetic photogrammetry, to analytical photogrammetry and to photogrammetric instrumentation.

References

Bennett, A. (1927), The Distortion of some Photographic Objectives. *Journal of the Optical Society of America*, Vol. 14, pp. 235–244.

Brown, D. (1956), The Simultaneous Determination of the Orientation and Lens Distortion of a Photogrammetric Camera. Air Force Missile Test Center Technical Report No. 56-20, Patrick AFB, Florida.

Brown, D. (1958), Photogrammetric Flare Triangulation, A New Geodetic Tool. Air Force Missile Test Center Technical Report No. 58-8, Patrick AFB, Florida.

Brown, D. (1959), Results in Geodetic Photogrammetry I. Air Force Missile Test Center Technical Report No. 59-25, Patrick AFB, Florida.

Brown, D. (1964), An Advanced Reduction and Calibration for Photogrammetric Cameras. Air Force Cambridge Research Laboratories Report No. 64-40.

Brown, Davis, Johnson (1964), The Practical and Rigorous Adjustment of Large Photogrammetric Nets. Rome Air Development Center Technical Documentary Report No. 64-353.

Carman, P. (1949), Photogrammetric Errors from Lens Decentering, *Journal of the Optical Society of America*, Vol. 39, pp. 951–954.

Conrady, A. (1919), Decentered Lens Systems, *Monthly Notices of the Royal Astronomical Society*, Vol. 79, pp. 384–390.

Hadgigeorge, G. (1965), Numerical Results from Geodetic Satellite (ANNA) Optical Data, 2nd Intl. Symp. on the Use of Artificial Satellites for Geodesy, Athens, Gr. 27 April–1 May.

Hardy and Perrin (1932), The Principles of Optics, p. 551, McGraw-Hill.

Livingston, R. (1951), Tangential Distortion in the Metrogon Lens, Engineer Research and Development Laboratories Report No. 1219, Fort Belvoir, Virginia.

Martin, L. C. (1958), *Technical Optics*, Vol. 1, p. 326, Pitman Publishing Corporation.

Pennington, J. (1947), Tangential Distortion and Its Effect on Photogrammetric Extension of Control. Photogrammetric Engineering, Vol. XIII, No. 1, pp. 135–142.

Sewell, E. (1952), Field Calibration of Aerial Mapping Cameras. Manual of Photogrammetry, Second Edition, American Society of Photogrammetry.

Sharp, J. (1959), Increased Accuracy of the Multiplex System, Photogrammetric Engineering, Vol. XV, No. 3.

Strong, J. (1958), Concepts of Classical Optics, p. 304. W. H. Freeman and Co.

Washer, F. (1941), Locating the Principal Point of Precision Airplane Mapping Cameras. *Journal of Research of the National Bureau of Standards*, Vol. 27, pp. 405–412.

Washer, F. (1957a), The Effect of Prism on the Location of the Principal Point. Photogrammetric Engineering, Vol. XXIII, No. 3, pp. 520–532.

Washer, F. (1957b), Prism Effect Camera Tipping, and Tangential Distortion. Photogrammetric Engineering, Vol. XXIII, No. 4, pp. 721–732.

——— (1965), Satellite Triangulation in the Coast and Geodetic Survey, USCGS Technical Bulletin No. 24.